Proceedings of the Institution of Civil Engineers
Ground Improvement 162
August 2009 Issue GI3
Pages 121–132
doi: 10.1680/grim.2009.162.3.121

Paper 800004
Received 14/01/2008
Accepted 12/11/2008

Keywords: land reclamation/densification/dynamics/granular soil




M. W. Bo
Director (Geo-Services), DST Consulting Engineers Inc., Thunder Bay, Ontario, Canada

Y. M. Na
Chief Engineer, Hyundai Engineering and Construction, Seoul, South Korea

A. Arulrajah
Senior Lecturer, Faculty of Engineering and Industrial Sciences, Swinburne University of Technology, Melbourne, Australia

M. F. Chang
Associate, Shannon & Wilson, Inc., USA.

Densification of granular soil by dynamic compaction

M. W. Bo DUC, MSc, PhD, FGS, FICE, CEng, CGeol, CEnv, CSci, PEng PGeo, EurGeol, EurEng, Y. M. Na MSc, PhD, PEng, A. Arulrajah MEng, PhD, CPEng, FIEAust and M. F. Chang MEng, PhD, PE

Land reclamation often involves the placement of loose granular soil by means of hydraulic filling. Sand fill formed by hydraulic filling generally does not allow densification by surface compaction methods because of their limited depth of influence. Loose granular soil is susceptible to liquefaction upon the impact of dynamic forces. Even under static conditions, loose granular soil may be subjected to bearing capacity failure and large settlements, because of its low shearing resistance and high compressibility. Various densification methods are used for improving such soils to increase the friction angle and elastic modulus. Several methods of deep compaction are available for such applications; among these, dynamic compaction is one of the most effective ways of densifying granular soils to a significant depth. However, the success of dynamic compaction is affected by many factors, several of which are not yet fully understood. This paper deals with the dynamic compaction densification method utilised at the Changi East reclamation site in Singapore for the improvement of reclaimed sand fill. Field data collected are used as a basis to investigate the effectiveness of the densification method and the effect of various influencing factors critical to the success of dynamic compaction treatment.

1. INTRODUCTION

Reclamation by means of hydraulic filling generally results in loose granular fill. In addition, the granular soil mass formed by hydraulic filling cannot be densified using surface compaction, which requires lift-by-lift application of compacting energy. Therefore deep compaction is often required.

Several methods of deep compaction are available for the densification of granular soils; among these, dynamic compaction is one of the effective methods for densifying granular soil in situ to a great depth. However, the success of dynamic compaction is affected by many factors, several of which are not yet fully understood. This paper describes the dynamic compaction densification method used at the Changi East reclamation site in Singapore for the improvement of reclaimed sand fill. Field data collected were used to investigate the effectiveness of the densification method and the effect of various influencing factors critical to the success of dynamic compaction treatment.

2. CHANGI EAST RECLAMATION PROJECT AND SAND FILL DENSIFICATION

The Changi East reclamation projects include 2000 ha of land reclamation, which was carried out under five phases because vast quantities of fill material and ground improvement were required. The project site was located in the eastern part of Singapore, as shown in Figure 1. A major portion of the site was reclaimed for future expansion of the Singapore Changi airport, and the remaining areas were for industrial and other usages.

These projects included an extensive amount of soil improvement works for treating the underlying compressible clay as well as the granular fill. The hydraulic fill at Changi consisted mainly of sand with less than 10% fines to a thickness of up to 20 m. The grain size distribution of the granular fill is shown in Figure 2.

As the granular fill was deposited by means of hydraulic filling using sand dredged from a borrow source, it was in a loose state, with the range of cone resistance falling between 5 and 7 MPa. In order to avoid excessive settlement of the fill, and to satisfy the requirements of runway pavement design, the cone resistance specified for the granular fill after densification was 15 MPa for the runway and 12 MPa for the taxiway areas: these are approximately equivalent to relative densities of 75% and 70% respectively.

An area of about 114 ha was improved by deep compaction methods covered granular fill 7 – 10 m thick. Three types of deep compaction method were deployed: dynamic compaction, vibroflotation and Muller resonance compaction (MRC) . The areas where the three different types of compaction method were used are shown in Figure 3. The dynamic compaction method was deployed in the area where the required depth of compaction was 5 – 7 m. The vibroflotation and MRC methods were adopted in the areas where the required thickness of compaction was 7 – 10 m.

Each of the three compaction methods has its own advantages and disadvantages, depending on the site and soil conditions in the various areas. Nevertheless, the specified degree of compaction was achieved in all areas. This paper emphasises the densification of granular fill by applying dynamic compaction.

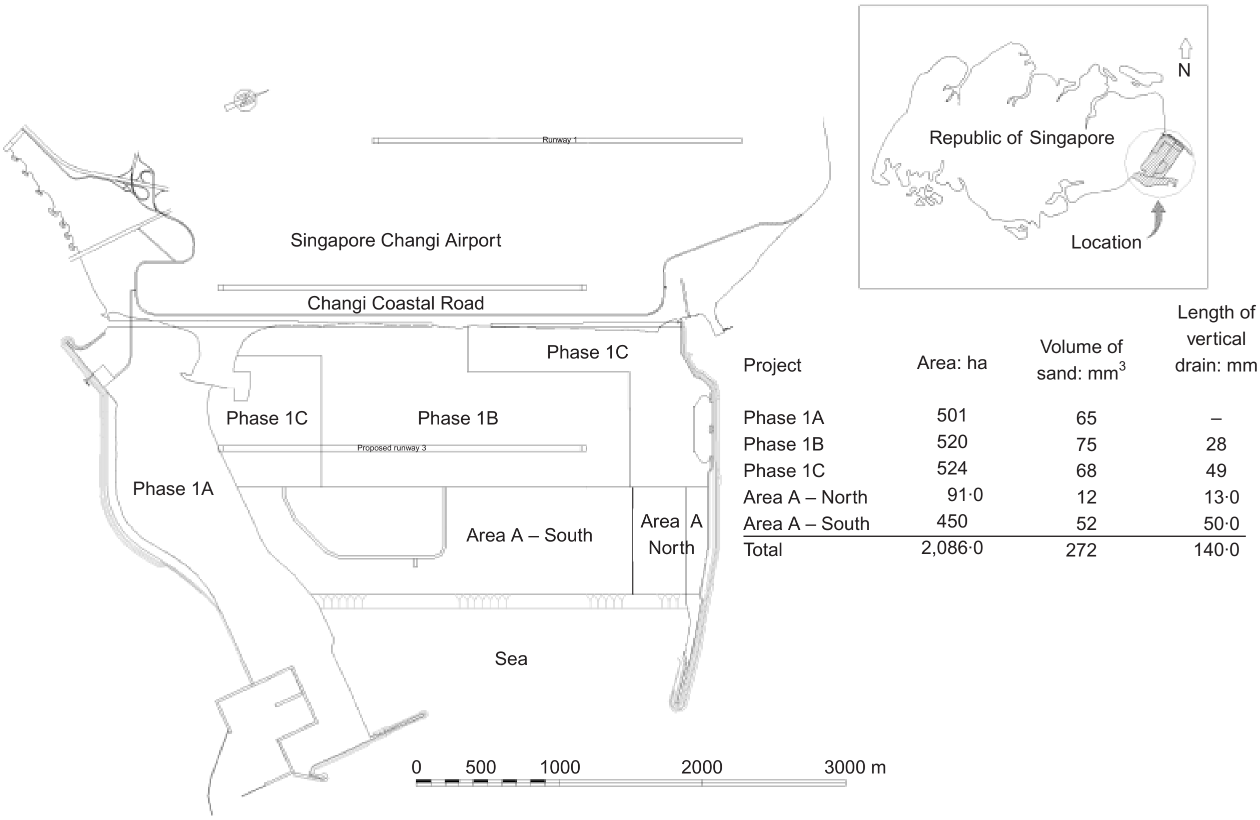

Project	Area: ha	Volume of sand: mm^3	Length of vertical drain: mm
Phase 1A	501	65	–
Phase 1B	520	75	28
Phase 1C	524	68	49
Area A – North	91·0	12	13·0
Area A – South	450	52	50·0
Total	2,086·0	272	140·0

Figure 1. Location of Changi East reclamation project

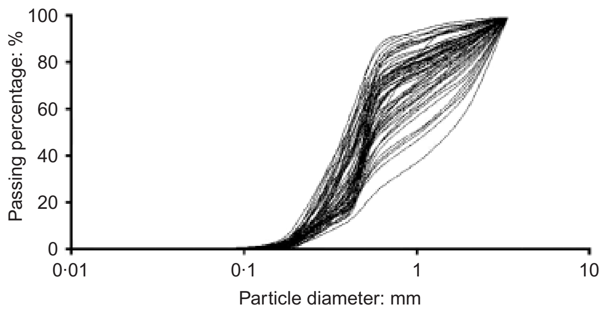

Figure 2. Grain size distribution of granular fill used in Changi East reclamation project

3. DETERMINATION OF DENSIFICATION REQUIREMENTS

3.1. Degree of densification

The densification requirements for a project are often ascertained based on the required bearing capacity, and/or the allowable magnitude of tolerable settlement. The bearing capacity of a shallow foundation is usually dependent upon the geometry of the foundation and shear strength parameters of the soil, especially the peak angle of shear strength (ϕ'). The magnitude of settlement is inversely proportional to the modulus of elasticity (E) of granular soil. It is desirable to avoid bearing failure, which can be achieved by improving the peak angle of shear strength of the granular fill, and to minimise settlement by enhancing the modulus of elasticity of the soil through deep densification treatment. In practice, however, it is not practical or economical to measure the in situ ϕ', and it is also difficult and time consuming to measure the value of E at various levels along the depth of a soil profile. In some projects the increase in modulus measured by pressuremeters is specified, but there are practical difficulties in measuring the modulus with pressuremeters in the sand. The required degree of densification can be specified in terms of relative density, in view of the fact that there is a strong correlation between the relative density of granular soil and its peak angle of shear strength and modulus of elasticity of granular soil. The required peak angle of shear strength and modulus of elasticity were determined based on acceptable settlement and bearing capacity requirements for the future loading expected on the improved land. The improved granular soil parameters after densification are generally measured by means of the standard penetration test (SPT) or the cone penetration test (CPT). Dynamic probing tests (DPT) were also frequently carried out for preliminary assessment of the increase in resistance. Relative density can be correlated with field measurements, such as those from SPT and CPT.[1–6]

3.2. Depth of compaction

Determination of the required densification depth is also critical for a densification project. If there is no design requirement for liquefaction (i.e. no anticipated seismic or dynamic forces), the densified granular soil mass is required only to meet bearing capacity and settlement criteria. In this case, the densification can be determined based on the estimated pressure bulb for a particular type and geometry of foundation. However, if liquefaction is a consideration, the depth of treatment required may increase significantly,

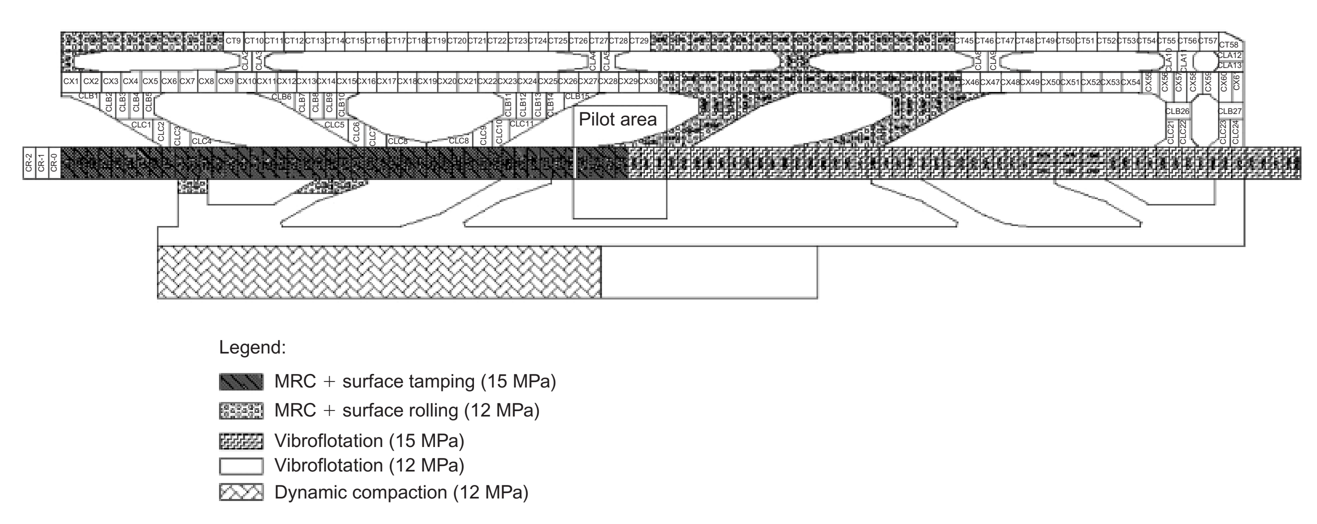

Figure 3. Layout showing areas where different methods of deep compaction were applied

depending on the liquefaction potential under the predicted dynamic and seismic forces.

4. DYNAMIC COMPACTION: CURRENT PRACTICE AND COMMON UNDERSTANDING

Dynamic compaction (DC) is a technique for improving the mechanical properties of granular soil at depths by repeatedly lifting and dropping a heavy weight (pounder) onto the ground surface. Repeated impacts over split-second durations are imparted to the granular soil when the heavy weight hits the ground surface. The impact energy causes the soil particles to be rearranged into a denser state. The selection of impact spacing and the number of drops per impact point is essential if the specified density is to be achieved.

The compaction process is usually repeated in several passes until the required post-treatment relative density has been achieved. The spacing for the first pass of impact points is usually equal to the thickness of the densifiable layer, in order to allow the impact energy to reach the lower part of the layer. The second pass is generally made at the centroid prints of the first pass. During each pass, several drops are made at the same point. There is a maximum number of impacts that leads to the closure of voids in order to achieve the minimum void ratio; after this there is usually no further closure of voids in the treated soil mass. After each pass, the craters created by the dropping pounder are usually backfilled with surrounding materials prior to the next pass. Finally, an ‘ironing’ pass with a low-energy impact and reduced drop height is performed to compact the shallow surface layer.

The basic mechanism underlying dynamic compaction in granular soils is relatively well understood. When the pounder impacts on the ground surface, the impact energy is transformed into seismic radiation, which subsequently transmits into the underlying soil mass. At the moment of impact with the pounder, the impact energy is transmitted mainly in body waves that consist of compression and shear waves, although surface waves are also generated in the soil. Whereas the body waves propagate radially outwards from the source along a hemispherical wavefront, as shown in Figure 4, the surface waves propagate horizontally along the surface. The influence of these shock waves on the soil is dependent on the soil types and the degree of saturation. For dry deposits the compressive and shear waves induced by the impact overcome the interlocking stresses within the loose strata, resulting in a reduction of voids. For a saturated granular deposit the mechanism of densification is quite different. The compressive stresses induced by the DC impact result in a sudden increase in pore water pressure, thereby forcing the soil into a state of temporary liquefaction. The shear waves and Rayleigh waves,

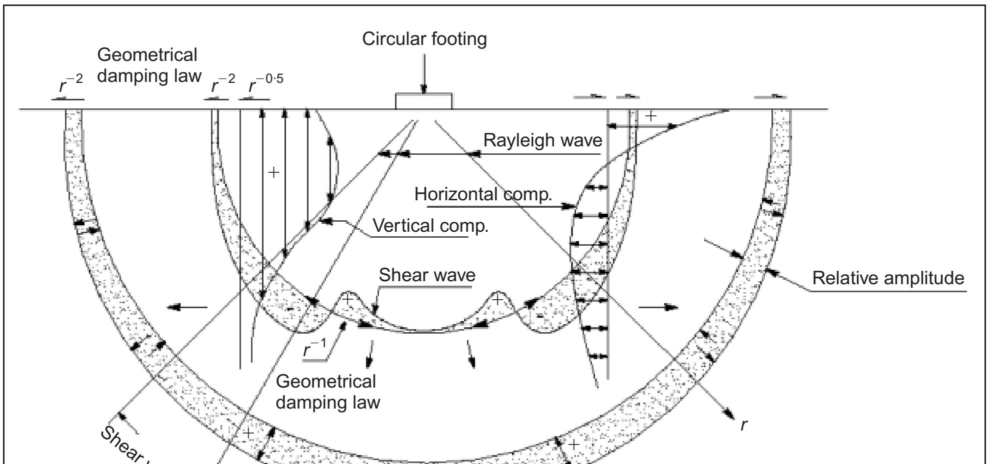

Figure 4. Wave propagation due to dynamic compaction[7]

which are slower, travel through the soil skeleton. The combination of a temporary loss of contact stresses and dynamic oscillation forces the soil particles to rearrange into a dense state.

4.1. Influence depth

The common understanding of dynamic compaction of granular soil is that the degree of improvement increases with the applied energy, and the influence depth increases with the pounder weight and drop height. The pounders are usually square, circular, hexagonal or octagonal in shape, and made of steel or concrete. Their weights normally range from 5 to 40 t, and drop heights could be up to 25 m. Menard and Broisc[8] proposed a formula that allowed an estimation of the influence depth D, in metres, as

$$D = (w \times h)^{1/2} \quad (1)$$

where w is the weight of the pounder in tonnes, and h is the drop height in metres. A more appropriate and accepted form of equation is given by Lukas[9] as

$$D = n(w \times h)^{1/2} \quad (2)$$

where n is an empirical coefficient factor that varies between 0·3 and 1·0. An n value of 0·5 was proposed by Leonards *et al.*[10] on the basis of compilation of field data for a number of conditions. The effectiveness of dynamic compaction is strongly affected both by the soil condition and by the energy configuration.

Van Impe[11] pointed out that the depth of influence depends upon the surface area and the shape of the pounder. Lukas[12] stated that multi-tamping improved only the zone of influence, and not the depth of influence. The degree of granular soil improvement by dynamic compaction peaks at a critical depth, which is roughly one half of the maximum depth of influence. Mayne *et al.*[13] proposed a useful correlation between the normalised crater depth, $D_c/(wh)^{1/2}$, and the number of drops.

Poran and Rodriguez[14] reported that there is a consistent relationship between the trial specific energy and the dimensions of the densifiable soil mass.

Based on numerical analyses, Chow *et al.*[15] proposed a method for predicting the crater depth by applying a wave equation model. They validated their predictions with two case studies, and found that their proposed method worked well.

5. INVESTIGATION AND OBSERVATIONS AT CHANGI

In order to investigate the effectiveness of the dynamic compaction and factors affecting influence depth and crater depth, a study was carried out at the Changi East reclamation site. The site was underlain by a recently reclaimed sand fill with an average thickness of 10–12 m. The granular soil has a D_{50} of 0·4 to 1 mm (Figure 2), and a narrow range of q_c, between 5 and 7 MPa (Figures 14 and 15). The soil was loose, but fairly homogeneous.

The results of numerous tests obtained from Changi during the early phases of reclamation suggest that the n factors for various energy weights and drop heights[16] vary from 0·33 to 0·44, similar to the value proposed by Leonards *et al.*[10] In this study, influence depth was determined from the CPT tests carried out after compaction. Table 1 shows that different n values are obtained using different pounders in Changi. It is worth noting that the depth of influence is also dependent upon the size and shape of the pounder. Data collected from Changi suggest that the same weight of pounder with the same energy may result in different influence depths if the geometry of the pounder is different.

From Equation 2, the required pounder weight and height of the drop can be selected to achieve the required depth of compaction. The effectiveness of dynamic compaction is dependent on the combination of weight and geometry of the pounder, the height of drop, the spacing, the number of drops, and the total compactive energy applied. Details of the equipment and the energy applied, together with the achieved densification in the dynamic compaction work carried out at Changi East, are summarised in Table 2.

5.1. Shape of pounder

Pounders of several different shapes, including square, hexagonal and circular, have been used in dynamic compaction. The thickness of pounders may also vary. Some pounders have foot studs, or nuts and bolts used to hold the steel plates together. Pounders are usually made up of steel plates, although a few consist of concrete block. Figure 5 shows two types of pounder used in the dynamic compaction works at Changi. Generally, a pounder with a smaller base area will penetrate deeper than a pounder with a larger base area. This creates additional depth of influence and vertical displacement in the soil, which will be discussed in the next section.

5.2. Lifting and dropping mechanism

In dynamic compaction work, lifting of the pounder is usually achieved by using a crane with a winch system. High-capacity cranes with various boom lengths are used in dynamic

	Pounder mass: t			
	15	14	23	23
Drop height: m	20	20	12·5	25
Pounder surface area: m^2	3·87	2·25	5·5	5·5
Energy: t–m	300	280	287·5	575
Influence depth: m	7·5	7	6	8
n*	0·433	0·418	0·354	0·334

* Determined from CPT.

Table 1. Value of n for various pounders (after Choa *et al.*[16])

	Scheme			
	1	2	3	4
Pounder weight: t	23	15	18	18
Drop height: m	25	20	24	24
No. of drops per pass	5	10	10	12
Energy per drop: t	575	300	432	432
Spacing at each pass: m^2	6 × 6	6 × 6	8·5 × 8·5	10 × 10
No. of passes	2	2	2	2
Effective area of improvement: m^2	5·5	3·87	3·4	3·4
Energy per m^2: t-m	160	166	120	105
Compacted depth: m	7	7	7	7
Cone resistance achieved: MPa	~15	~15	~12	~12

Table 2. Details of dynamic compaction at Changi

compaction works. However, if the pounder is too heavy, tripods will need to be used instead of cranes. The drop point is just in front of the crane, or at the centre of the tripod. Figure 6 shows a crane and a tripod used in the dynamic compaction works at Changi East. In most cases, the cable follows with the pounder when the pounder is released. Significant friction between the pulley and cable can be expected, resulting in some energy losses. This is taken into account in the empirical coefficient *n* in Equation 2.

A system that allows the pounder to drop freely without significant energy losses from friction was also used in an early phase of the Changi East reclamation project. It comprises a clip holder, as shown in Figure 7. Figure 8 shows two types of pounder used at Changi East. Even in free-fall situations, energy losses arising from friction caused by rapid movement of the pounder in the air can still be expected. Figure 9 shows how the measured deceleration, velocity, vertical displacement and input stress compared with the calculated values.

The theoretical impact velocity of a falling pounder, v_1, can be calculated as

$$v_1 = \int a_t \mathrm{d}t + C_\mathrm{v} \quad (3)$$

where a_1 is the deceleration, t is the elapsed time and C_v is an integration constant.

The impact stress (σ_t) applied by the pounder over the duration of the impact can be calculated using the measured deceleration record, as

$$\sigma_t = \frac{ma_t}{A_0} \quad (4)$$

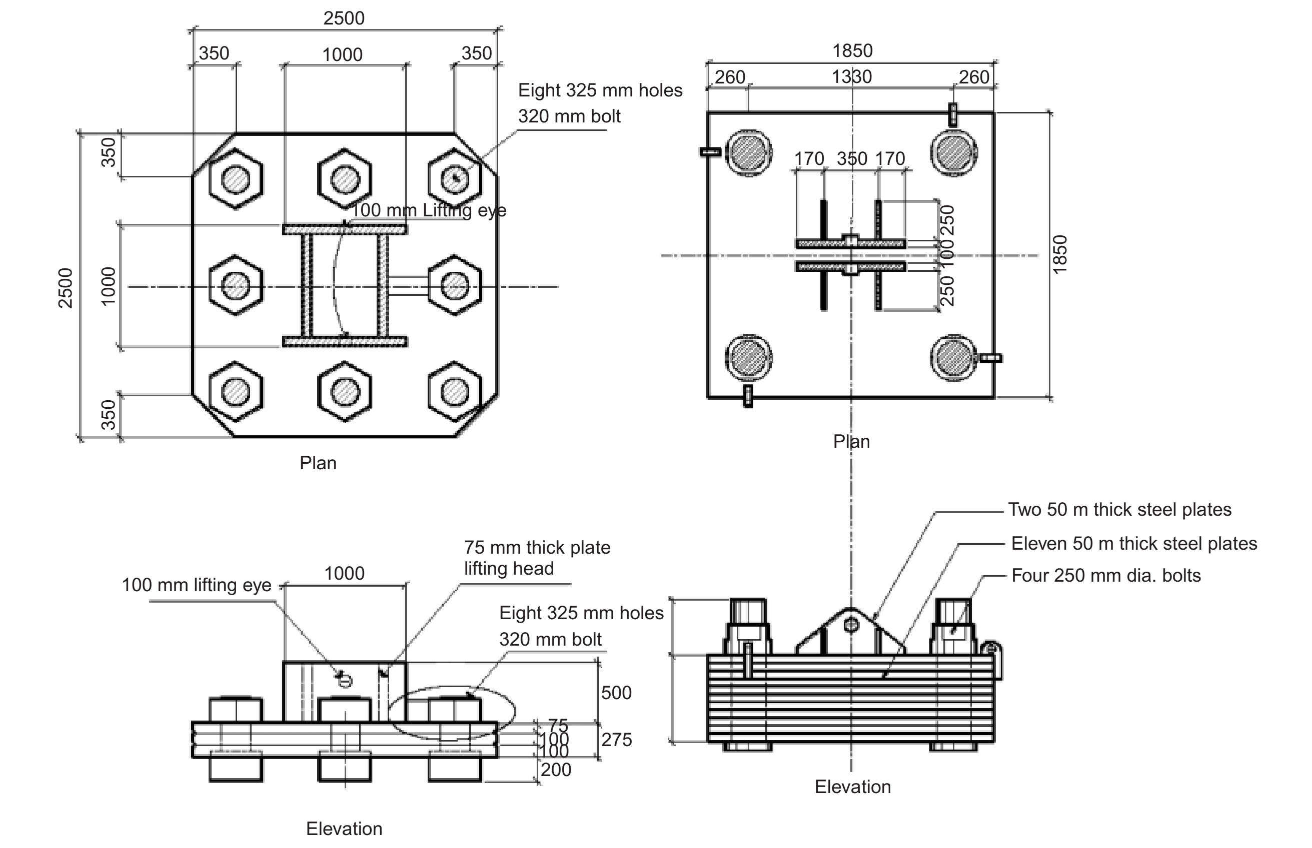

Figure 5. Geometry of two pounders used at Changi (dimensions in mm)

(a) (b)

Figure 6. (a) Crane and (b) tripod used at Changi

Figure 7. Lifting mechanism with clip holder

where m and A_0 are the mass and contact area of the pounder respectively.

Several different field measurements were made at the Changi reclamation project to check the energy losses, surface vertical displacement, and input stress and pore pressure due to dynamic compaction in the sand. Figure 9 shows a comparison of the theoretical and measured velocity of the pounder at the moment when it touches the surface. It can be seen that the measured velocity is typically about 80% of the theoretical velocity.

5.3. Vertical displacement induced by pounding

The vertical displacement of the pounder, or the crater depth, can be estimated. For example, the impact of an 18 t pounder dropped from 10 m height is about 1200 kPa. By integrating the calculated velocity (v_1), the displacement of the pounder (s_t) can be estimated from Equation 5. Figure 10 shows a comparison of the measured and estimated pounder vertical displacement, which is found to be comparable with that calculated from the following equation

$$s_t = \int v_1 \mathrm{d}t + C_\mathrm{d} \qquad (5)$$

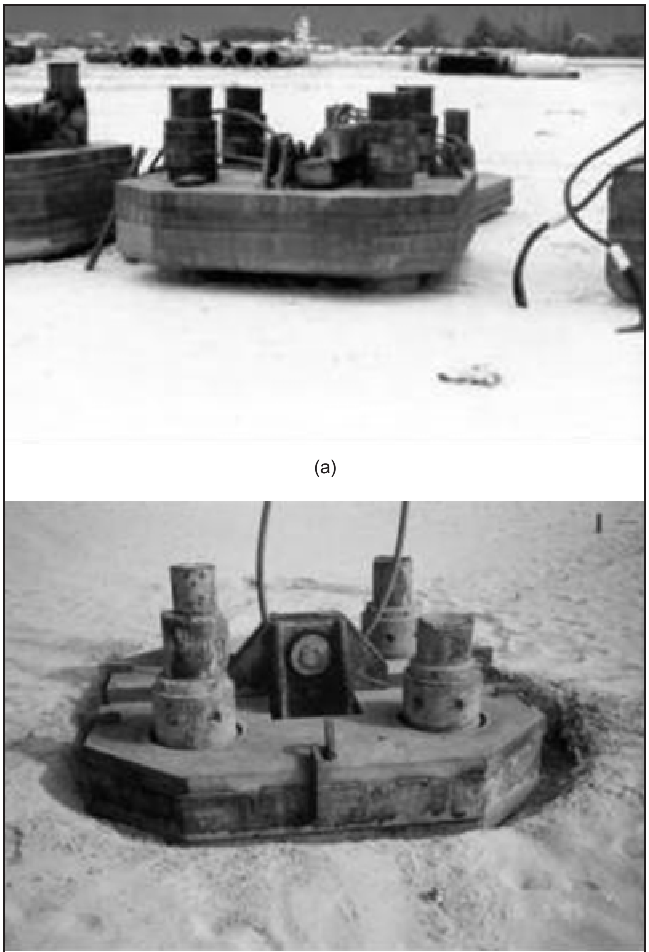

(a)

(b)

Figure 8. Two types of pounder used at Changi

where s_t was determined based on the actual 'at rest' incremental pounder displacement for each drop. Chow *et al.*[5] also have demonstrated that the crater depth caused by pounder displacement can be estimated by applying wave equation analyses.

Figure 11 shows a typical relationship between the peak impact deceleration and the drop number. For a pounder of 18 t dropping from a height of 10 m height for various numbers of drops, it was found that the deceleration peaked at the third drop. After the sixth drop it was maintained at a constant calculated deceleration. This means that after the sixth drop the effectiveness of subsequent compaction diminishes. The pounder vertical displacement was also found to approach a final stable value of 0·5 m shortly after the number of drops reached six.

5.4. Pore pressure response in soil

Pore water pressures in the soil mass at a depth of 5 m at two locations, 2 and 3 m from the pounder drop point, were measured during a trial test. It was found that a piezometer 2 m away recorded an excess pore pressure of about 140 kPa, and that at 3 m away 60 kPa was recorded (Figure 12). These pore pressures are almost ten times smaller than the impact stresses imposed at the fill surface. The excess pore pressure was found to increase in two cycles. First, the peak magnitude of excess pore pressure registered within less than 0·2 s, and dissipated immediately. Then the excess pore pressure again

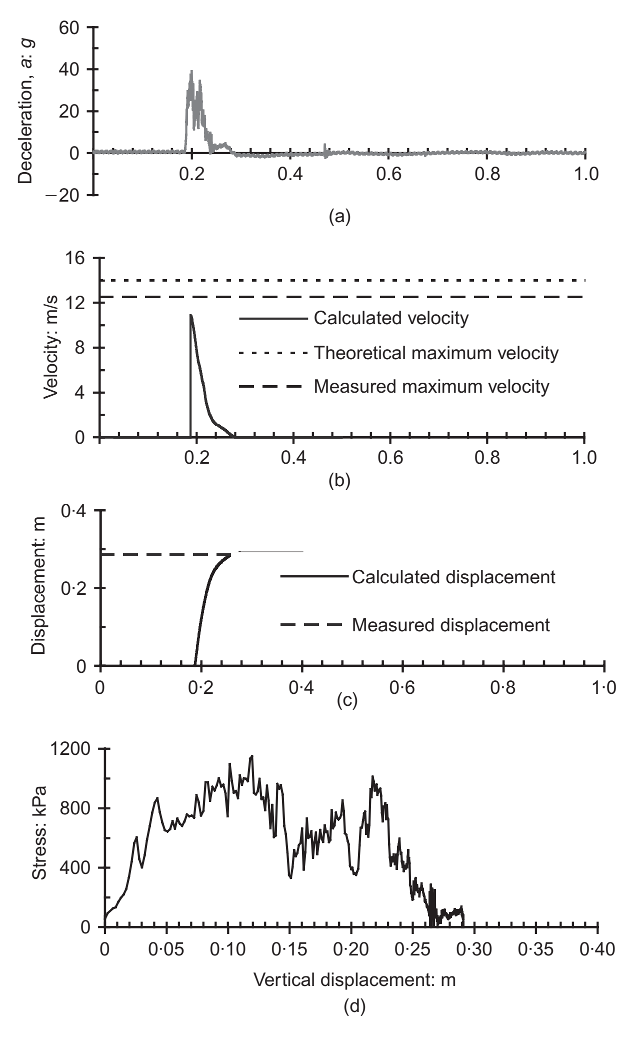

Figure 9. (a) Measured deceleration; (b) velocity measurement; (c) displacement; (d) stress. Drop height = 10 m; drop mass = 18 t; drop number = 1

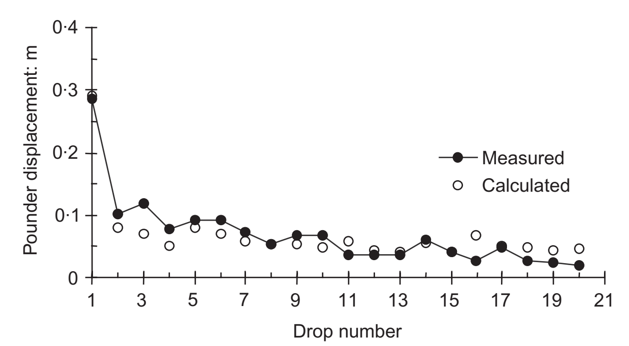

Figure 10. Comparison of measured and calculated pounder displacement

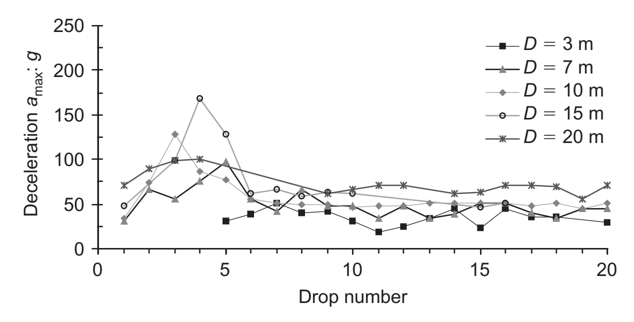

Figure 11. Deceleration measurement after pounder drops

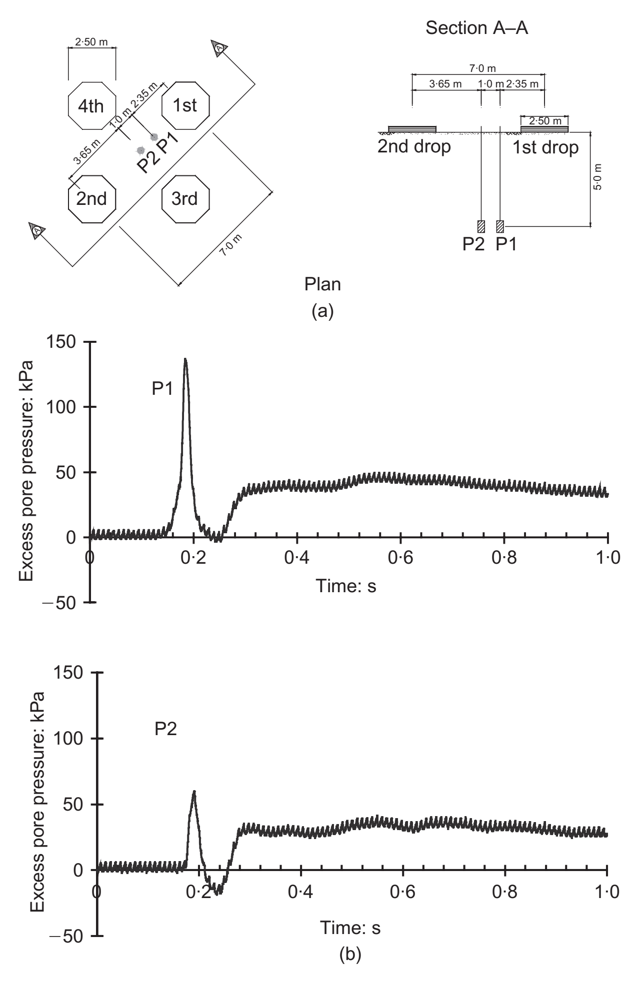

Figure 12. (a) Layout of measurement points; (b) measured excess pore pressure against time

increased, to a smaller magnitude that generally took 2–3 min to dissipate fully. In general it takes 3–4 min to complete the lifting and dropping process of dynamic compaction. Therefore, for dynamic compaction in granular soil excess pore pressure may not be a significant issue. Excess pore pressures were measured after varied rounds of pounding: it was found that the excess pore pressure increases with increasing number of drops. This can be attributed to increasing densification or, in other words, reduced void ratio of the granular soil after each drop.

5.5. Degree of improvement

In the design of densification work, selection of the required spacing and number of drops per point is essential in order to achieve the specified density requirement, as both factors affect the total compaction energy per unit surface area. Leonards *et al.*[10] reported that the degree of compaction correlated well with the energy product, which equated to the total energy applied per unit surface area times the energy per drop. Test results at Changi East, as shown in Figure 13, support Leonard's findings. The upper bound of maximum attainable cone resistance (q_c) is about 180 kg/cm^2 (18 MPa) for the soil in Changi, as illustrated in Figure 13.

In the Changi East reclamation project, energy products of 92 000 and 48 900 m^{2}t^2 were applied in order to attain maximum cone resistances of 18 MPa (180 kg/cm^2) and 12 MPa (120 kg/cm^2) respectively. The effective spacing of the pounding points and the numbers of drops per point calculated for particular pounders and cranes are shown in Tables 3 and 4. To achieve the selected effective spacing, the sequence of pounding can be arranged into two or more passes to allow for significant pore water pressure dissipation between passes.

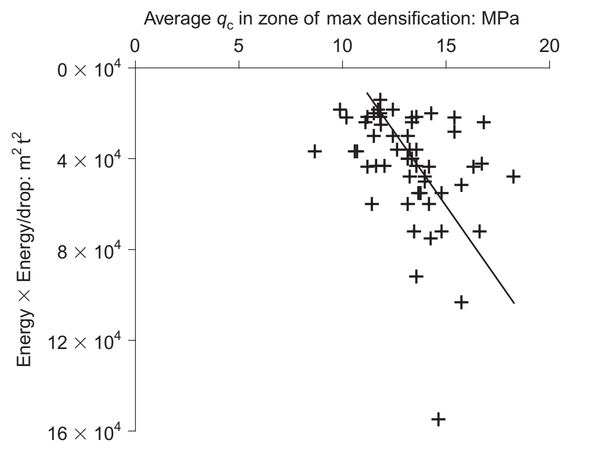

Figure 13. Correlation between average cone resistance and energy/m^2 times energy/drop

Several trial compaction tests were carried out with spacing between 6 and 10 m with various combinations of energy (Table 2). Based on these results, a spacing of 6 m by 6 m square was eventually used in the Changi East reclamation project. In both methods two passes of 6 m by 6 m spacing were applied, with drop point in the second pass at the centre of the first pass. Therefore the net effective area of treatment (i.e. the compacted area covered by one drop point after two passes) becomes 17·97 m^2, as shown in Table 4. Two methods, termed method A and method B, were applied using intensities of energy per drop of 575 and 300 t m respectively. These energy levels were achieved using 23 t and 15 t pounders dropped from 25 and 20 m and repeated for 5 and 10 drops respectively. Methods A and B were applied respectively for areas where the specified q_c was 15 and 12 MPa. The resulting q_c profiles after compaction are shown together with those prior to compaction in Figures 14 and 15 for methods A and B respectively.

In the study, several combinations of types of pounder and drop height under various soil conditions were used. For the same pounder and the same initial soil condition, the trend of the relationship between the normalised crater depth and the number of drops is similar, regardless of the drop height or the location of drops. This can be seen in Figures 16 and 17.

Also, for the same drop weight with the same pounder and the same drop height, the trend of normalised crater depth against number of drops may vary if the initial soil condition is different. Figure 18 shows the different trends observed after the first pass and the second pass using the same energy per drop. The crater depths are smaller with the same number of blows in the second pass, as the soil has been densified to a certain degree after the first pass of pounding.

Step		Method	
		A	B
1	Required CPT q_c: MPa	18	15
2	Pounder mass: t	23	15
3	Drop height: m	25	20
4: 2 × 3	Available energy per drop: t-m	575	300
5: Figure 12	Energy/m^2 × Energy/Drop: t^2	92 000	48 900
6: 5/4	Required energy/m^2: t-m/m^2	160	163
7: 4/6	Effective area/Drop: m^2	3·59	1·84

Table 3. Calculation of effective area

Step		Method	
		A	B
1	First pass effective: m^2	36	36
2	Second pass effective: m^2	36	36
3	Net effective area:* m^2	17·97	17·97
4: Table 2	Effective area/Drop: m^2	3·59	1·84
5: 3/4	Required no. of drops/Pass	5	10

* Net effective area after both passes (i.e. 6 m × 6 m square spacing, two passes).

Table 4. Calculation of required number of drops

For pounders of different geometries, the trend of normalised crater depth may vary, even if pounders of similar weight, dropping from the same height, are applied in the same type of soil. This can be seen in Figure 19. The information gathered at Changi is useful for guiding site supervision, since the trend of the normalised crater depth against the number of drops is independent of the drop height for the same pounder, as long as the base area is the same. So direct supervision can be kept to a minimum, done solely by the measurement of crater depth after pounding. Physical counting of the number of drops and observation of drop heights may not be required during the field observation, once the trial tests have been carried out on

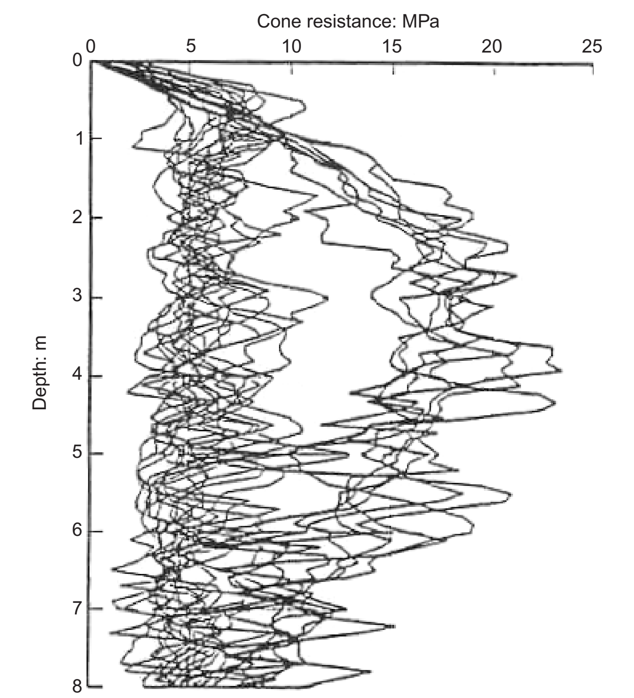

Figure 14. Pre- and post-compaction q_c profiles from method A

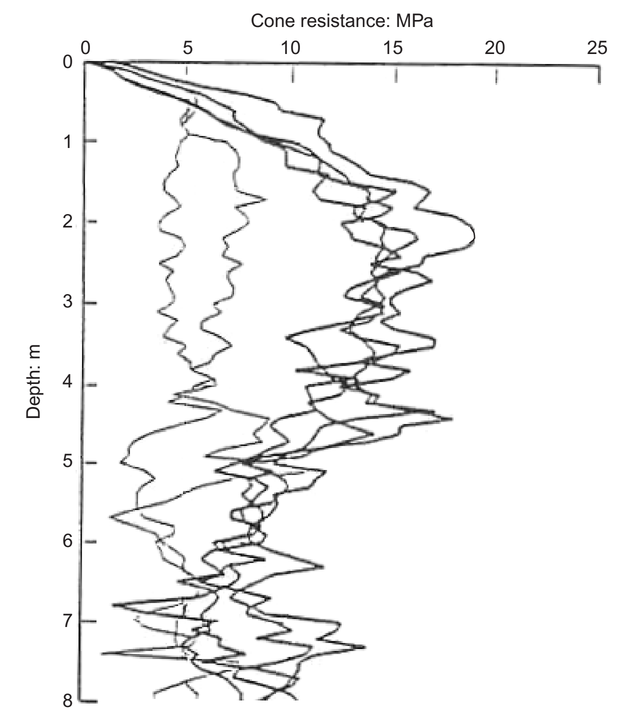

Figure 15. Pre- and post-compaction q_c profiles from method B

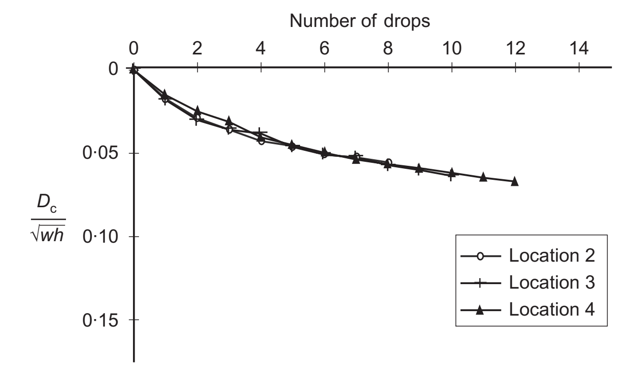

Figure 16. Normalised crater depths at different locations for a given energy per drop: $w = 15$ t; $h = 15$ m; D_c is in metres

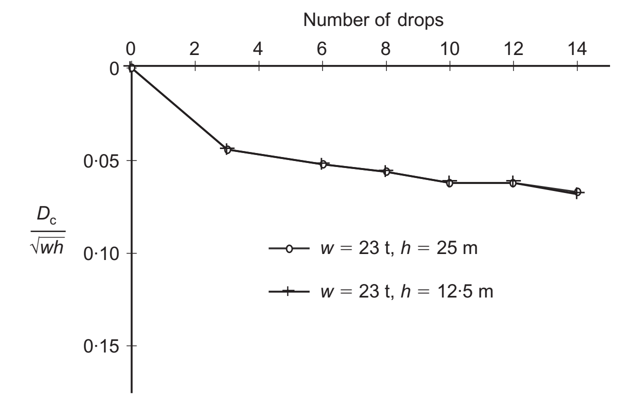

Figure 17. Normalised crater depths for different drop heights: D_c is in metres

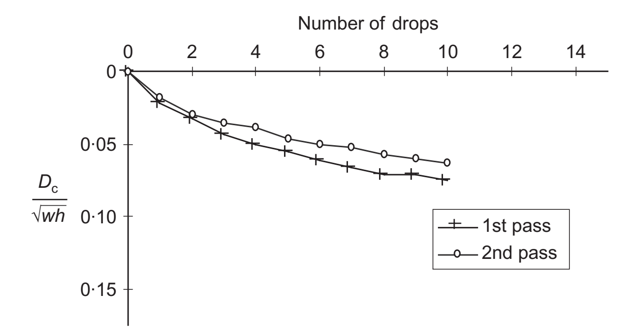

Figure 18. Normalised crater depths measured after first and second passes for the same energy per drop: $w = 15$ t; $h = 20$ m; D_c is in metres

the particular granular soil type to establish the relationship between the normalised crater depth and the number of drops.

5.6. Most compacted point

Most specifications in a dynamic compaction contract require that verification for acceptance of the compaction works be based on an in situ test performed at the centroid point, on the assumption that soil at the centroid location is the least compacted. However, if a correct spacing is used, the centroid point often turns out to be the most compacted point, and the location exactly under the pounder is actually the least compacted point.

Chow *et al.*[17] proposed the use of an improvement ratio, which is defined resistance expressed as function of the ratio of the peak angles of shear at any point in the soil and that underneath the pounder ($\Delta\Phi/\Delta\Phi_b$) ratio X/D. In their proposal $\Delta\Phi$ represent, the extent of improvement at a distance X from the centre of impact, $\Delta\Phi_b$ is that underneath the pounder and D is the diameter of the pounder. According to Chow *et al.*,[17]

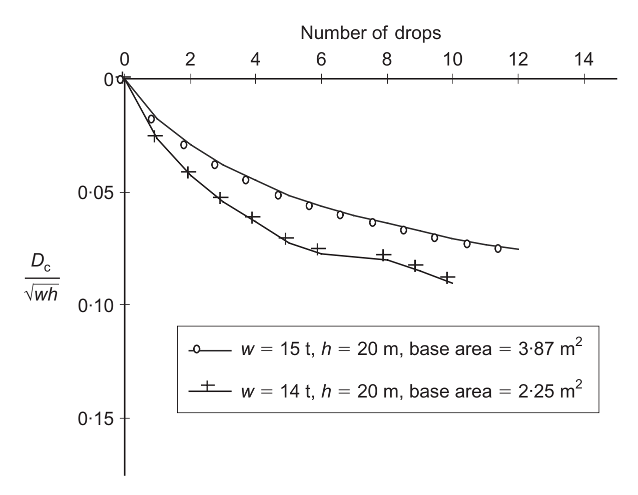

Figure 19. Normalised crater depths measured with similar pounder weights and drop heights but different base areas

the extent of improvement can be taken as zero at $X/D > 3{\cdot}5$ and 1·0 at $X/D \leqslant 0{\cdot}5$.

In the Changi East reclamation project, large numbers of CPTs were carried out around and under the pounder locations for 6 m by 6 m and 7 m by 7 m square grid spacings, both with two passes of pounding. In these tests, the X/D ratios of the centroid locations are between approximately 1·5 and 1·75. Selected comparative q_c profiles for various distances from the pounding points are shown in Figures 20 and 21. In general, at the location under the pounder point, the average q_c value is the lowest and the soil is the least compacted, although a thin layer of highly compacted sand between 2 and 3 m deep is present. The soils at the centroid point were found to be the most homogeneously compacted with depth. Sample plots of the contour of average values of relative density under the pounding point and the centroid point obtained from several measurements at the Changi project are shown in Figure 22. The relative densities shown in the figures were calculated based on the in situ measured densities and the maximum and minimum dry densities measured in the laboratory for representative samples. Note that, for the single pounding, the degree of densification reduces as the distance from the pounding point increases. However, for the multiple pounding, the soil mass located at the centroid of the compaction grid is generally well compacted owing to multiple pounding effects from all four adjacent pounding points if the correct grid pattern is applied. From Chow *et al.*'s predicted contours for X/Ω of 2·5 and 4,[17] a greater extent of improvement was achievable at the centroid point, where X/D becomes smaller. Therefore the centroid point may not be necessarily the ideal point for verifying the extent of improvement.

5.7. Ageing effect

Dynamic compaction is often carried out in passes to allow for pore pressure dissipation during the pause period. However, because granular soil is highly permeable, dissipation of excess pore pressure is generally quite rapid, particularly if fissures develop. Therefore no significant increase in strength or softening or ageing is expected after compaction. A minor increase in cone resistance may occur as a result of the slow redeposition of soluble silica at grain contacts, which act as natural cementation. Increases in penetration resistance over time after a densification treatment have been reported.[18–20] Schlosser[21] has proposed a method for estimating increased q_c after compaction. In the Changi East reclamation project CPTs were carried out at 14 days and 3 months after compaction, but the change in the cone resistance is scarcely noticeable (Figure 23). Most ageing, if indeed such an effect exists, should have taken place during the first 14 days.

6. CONCLUSIONS

Field measurements and observations from dynamic compaction used for the densification of hydraulically placed

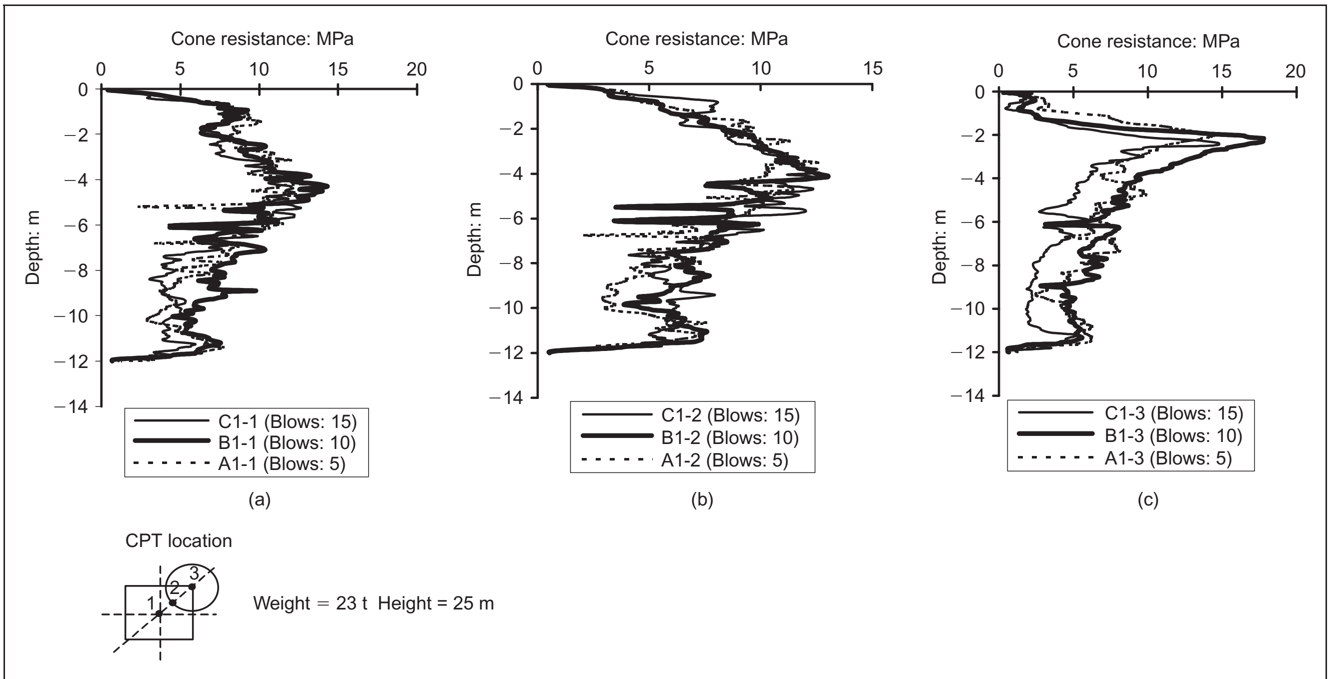

Figure 20. Cone resistance measured at various locations for 6 m × 6 m grid spacing: (a) centroid point; (b) intermediate point; (c) under the imprint

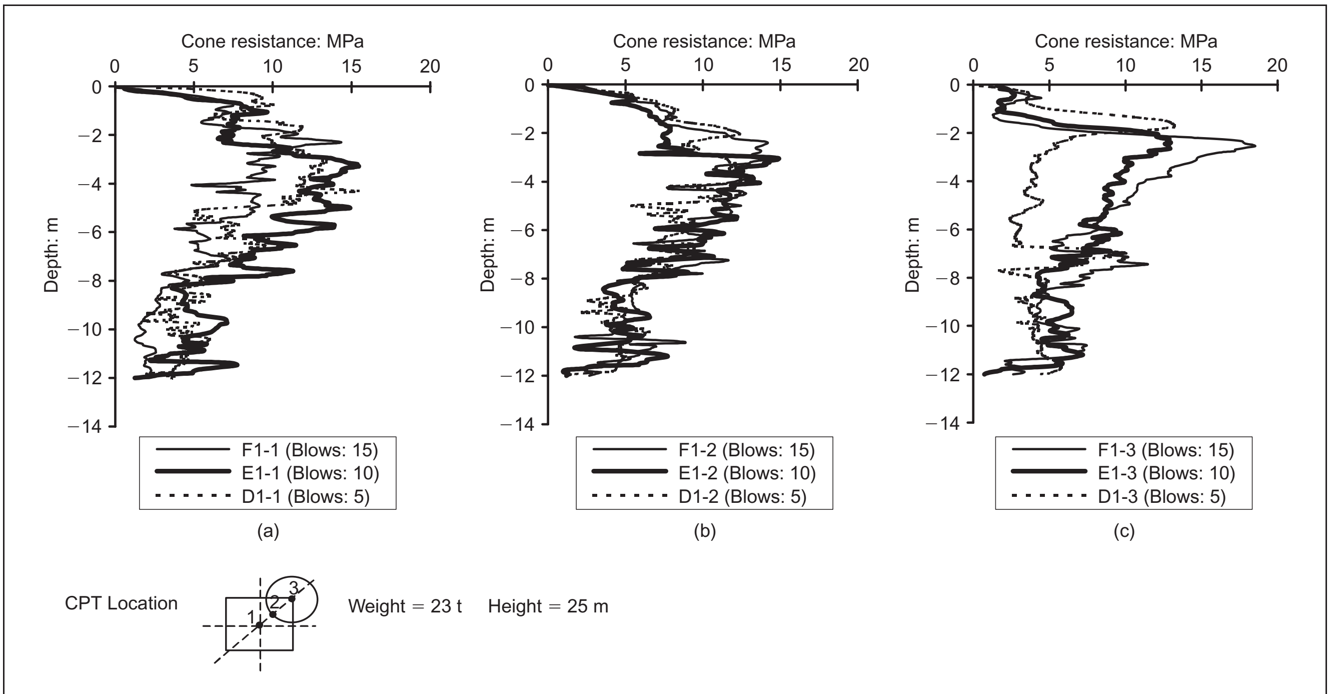

Figure 21. Cone resistance measured at various locations for 7 m × 7 m grid spacing: (a) centroid point; (b) intermediate point; (c) under the imprint

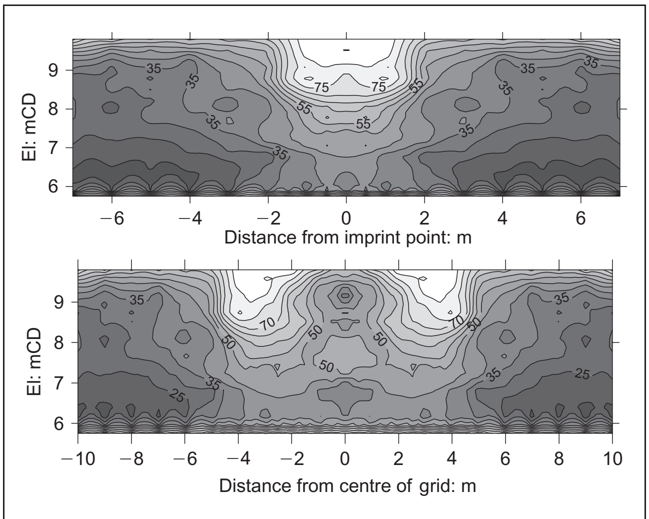

Figure 22. Contour of relative density under imprint and centroid points from several tests at Changi[22]

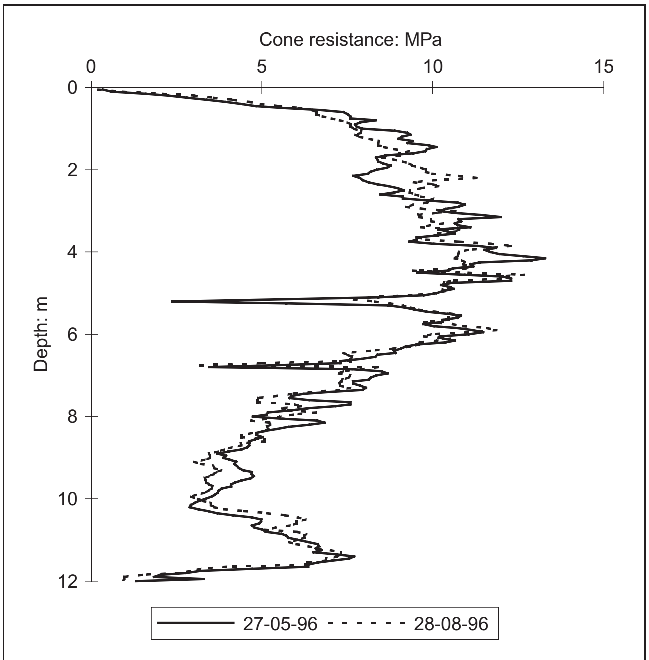

Figure 23. No significant ageing after 14 days of compaction

sandfill in the Changi East reclamation project have been described. Factors such as the degree of improvement, the most compacted point and the ageing effect have been investigated, based on field data collected in the project.

The following conclusions can be drawn.

(*a*) The centroid point within a compaction pattern is the most well-compacted point, and that directly under the pounder is often the least compacted. Therefore the centroid point should not be used as a quality control point.
(*b*) The influence depth can be estimated by applying the well-established generalised empirical correlation, although the components of the equation can be slightly different depending upon the geometry of pounder and the dropping mechanism. Suitable spacing, the required energy and the number of passes can also be estimated from the same empirical correlation.
(*c*) The geometry of the pounder and the initial soil conditions also affect the depth of the crater.
(*d*) No significant ageing effect was found more than 14 days after compaction at the Changi East site.
(*e*) Physical counting of the number of drops and observation of drop heights may not be required during the field supervision of dynamic compaction once trial tests have been carried out on a particular granular soil type to establish the relationship between the normalised crater

depth and the number of drops. The role of direct supervision during actual work can in practice be replaced by the measurement of crater depth after pounding.

REFERENCES

1. JAMIOLKOWSKI M., LADD C. C., GERMAINE J. T. and LANCELLOTTA R. New development in field and laboratory testing of soils. *Proceedings of the 11th International Conference on Soil Mechanics and Foundation Engineering, San Francisco*, 1985, 1, 57–153.
2. SKEMPTON A. W. Standard penetration test procedures and effects in sands of overburden pressure, relative density, particle size and overconsolidation. *Journal of Geotechnical Engineering*, 1986, **112**, No. 3, 425–447
3. SALGADO R., MITCHELL J. K. and JAMIOLKOWSKI M. Cavity expansion and penetration resistance in sand. *Journal of Geotechnical and Geoenvironmental Engineering, ASCE*, 1997, **123**, No. 4, 344–354.
4. CUBRINOVSKI M. and Ishihara K. Empirical correlation between SPT N-value and relative density of sandy soils. *Soils and Foundations*, 1999, **39**, No. 5, 61–71.
5. CHOW Y. K., YONG D. M., YONG K. Y. and LEE S. L. Dynamic compaction of loose sand deposits. *Soils and Foundations*, 1992, **32**, No. 4, 93–106.
6. BALDI G., BELLOTTI R., GHIONNA V., JAMIOLKOWSKI M. and PASQUALINI E. Interpretation of CPTs and CPTUs. Part 2: Drained penetration. *Proceedings of the 4th International Geotechnical Seminar, Singapore*, 1986, 143–156.
7. WOODS R. D. Severing of surface wires in soils. *Journal of Soil Mechanics and Foundation, ASCE*, 1968, No. SM4, DSI-098.
8. MENARD L. and BROISE Y. Theoretical and practical aspects of dynamic consolidation. *Géotechnique*, 1975, **25**, No. 1, 3–18.
9. LUKAS R. G. Dynamic compaction: engineering considerations. In *Grouting, Soil Improvement and Geosynthetics*, ASCE Geotechnical Special Publication No. 30, Vol. 2, ASCE, New York, 1992, pp. 940–953.
10. LEONARDS G. A., CUTTER W. A. and HOLTZ R. D. Dynamic compaction of granular soils. *Journal of the Geotechnical Engineering Division, ASCE*, 1980, **106**, No. 1, 35–44.
11. VAN IMPE W. F. *Soil Improvement Techniques and Their Evolution*. A. A. Balkema, Rotterdam, 1994.
12. LUKAS R. G. *Dynamic Compaction for Highway Construction: Design and Construction Guidelines*, US Department of Transportation, 1986, Report No. FHWA/RD-86/133.
13. MAYNE P. W., JONES J. S. and DUMAS J. C. Ground response to dynamic compaction. *Journal of Geotechnical Engineering, ASCE*, 1984, **110**, No. 6, 757–774.
14. PORAN C. J. and RODRIGUEZ J. A. Design of dynamic compaction. *Canadian Geotechnical Journal*, 1992, **29**, No. 5, 796–802.
15. CHOW Y. K., YONG D. M., YONG K. Y. and LEE S. L. Dynamic compaction analysis. *Journal of Geotechnical Engineering, ASCE*, 1992, **120**, No. 8, 1141–1157.
16. CHOA V., BO M. W., ARULRAJAH A. and NA Y. M. Overview of densification of granular soil by deep compaction methods. *Proceedings of the International Conference on Ground Improvement Techniques*, Macau, 1997, pp. 131–140.
17. CHOW Y. K., YONG D. M., YONG K. Y. and LEE S. L. Dynamic compaction of loose granular soils: effect of print spacing. Improvement of granular soils by high energy impact. *Journal of Geotechnical Engineering, ASCE*, 1994, **120**, No. 7, 1115–1133.
18. DEBATS J.-M. and SIMS M. Vibroflotation in reclamation in Hong Kong. *Ground Improvement*, 1997, **1**, 127–145.
19. MITCHELL J. K. Soil improvement: state of the art report. *Proceedings of the 10th International Conference on Soil Mechanics and Foundation Engineering, Stockholm*, 1981, **4**, 509–565.
20. OSHIMA A. and TAKADA N. Relation between compacted area and ram momentum by heavy tamping. *Proceedings of the 14th International Conference on Soil Mechanics and Geotechnical Engineering, Hamburg*, 1997, **3**, 1641–1644.
21. SCHLOSSER F. Theme lecture: Soil improvement and reinforcement. *Proceedings of the 14th International Conference on Soil Mechanics and Geotechnical Engineering, Hamburg*, 1997, **4**, 2445–2466.
22. NYM. Institution characterization of reclaimed sandfill with particular reference to dynamic compaction, Thesis Mangory Technology University, Singapore, 2002.

What do you think?
To comment on this paper, please email up to 500 words to the editor at journals@ice.org.uk

Proceedings journals rely entirely on contributions sent in by civil engineers and related professionals, academics and students. Papers should be 2000–5000 words long, with adequate illustrations and references. Please visit www.thomastelford.com/journals for author guidelines and further details.